Journal of Engineering Mathematics (2005) 51: 211–230
DOI 10.1007/s10665-004-6091-5

Large deformation of shear-deformable plates by the boundary-element method

J. PURBOLAKSONO and M.H. ALIABADI[1,*]
Department of Engineering, Queen Mary, University of London, Mile End Road, London E1 4NS, United Kingdom; [1]*Department of Aeronoatics, Imperial College, London, South Kensingdon, London SW7 2BY, United Kingdom* **Author for correspondence (m.h.aliabadi@imperial.ac.uk)*

Received 11 September 2003; accepted in revised form 9 November 2004

Abstract. Boundary-integral equations for large deformation of shear-deformable plates are presented. Two different methods are used to calculate the derivatives of the nonlinear terms in the domain integral. The first approach requires the evaluation of a hypersingular domain integral. The second approach avoids the calculation of a hypersingular integral by utilizing radial basis functions to approximate the integrand. Quadratic isoparametric boundary-elements are used to discretise the boundary, and constant cell elements are used to discretise the domain. For the solution of a nonlinear problem four methods are presented. They include: total incremental method, cumulative-load incremental method, Euler method and nonlinear system method. Several examples are presented and comparisons with analytical results and other numerical results are made to demonstrate the accuracy of the proposed methods.

Key words: boundary-element method, large deformation, shear-deformable plate

1. Introduction

Geometrically nonlinear behaviour in solid mechanics is an important problem in engineering practice. The bending of rectangular plates with large deflection was studied by Levy [1,2] by solving the von Kármán equation in terms of trigonometric series. An approximate analysis of the large deflection for plates was introduced by Berger [3], which culminated in the well-known Berger equation. The first application of the boundary-element method (BEM) to classical plate theory can be traced to the work of Jaswon, Maiti and Symm [4]. The application of the direct BEM for analysis of the Reissner plate was presented by Vander Ween [5]. Later, Karam and Telles [6] extended the formulation to account for infinite regions. Rashed, Aliabadi and Brebbia [7,8] presented a BEM formulation for Reissner plates resting on Pasternak and Winkler foundations. Wen, Aliabadi and Young [9] presented a boundary-only formulation for shear-deformable plates and shells using the dual reciprocity method. The application of the boundary-element method to large nonlinear deformation is relatively new, with only a few publications dealing with this topic. Tanaka [10] presented a coupled boundary and inner-domain integral equation in terms of stress and displacement functions based on von Kármán's equation. Kamiya and Sawaki [11] investigated the large deflection of elastic plates based on the Berger equation. Ye and Lin [12] analysed the finite deflection of a thin plate by the boundary-element method. Based on the general nonlinear differential equations describing the finite deflection of the plate, an integral equation formulation for the geometrically nonlinear analysis of a Reissner-type plate was proposed by Lei, Huang and Wang [13]. Later, Sun, He and Qin [14] derived the exact boundary equation for a nonlinear

Reissner plate based on a variational principle. Other contributions can be found in the papers by Sladek and Sladek [15], Katsikadelis [16] and Atluri and Pipkins [17].

A hypersingular boundary-element formulation for Reissner-plate bending was presented by Rashed, Aliabadi and Brebbia [18], a dual boundary-element method for analysis of fracture-mechanics problems was developed by Wen, Aliabadi and Young [19] and, Dirgantara and Aliabadi [20]. A comprehensive review of BEM formulation is given by Aliabadi [21,22]. In the analysis of geometrically nonlinear plate-bending problems, one of the difficulties concerns the evaluation of domain integrals in the boundary-integral equations, coupling the plate-bending and membrane terms. In this paper, the derivation and implementation of domain boundary-integral equations for the large deformation of shear-deformable plates are presented. The domain integrals that appear in the formulation are treated in two different ways: firstly, they are evaluated as hypersingular integrals, and secondly, an approximation function is used to calculate the derivatives of the nonlinear terms in the domain integral. Four different methods are investigated for the solution of the nonlinear problem. They include methods requiring increments of the load and a method based on the solution of the nonlinear system of equations. Several examples are presented, and comparisons with analytical results and other numerical results made, to demonstrate the accuracy of the proposed methods.

2. Governing equations

The equations governing the deflection of geometrically nonlinear plates (see Figure 1) can be written in compact form, using indicial notation, as follows

$$M_{\alpha\beta,\beta} - Q_\alpha = 0, \tag{1}$$

$$Q_{\alpha,\alpha} + (N_{\alpha\beta} w_{3,\beta})_{,\alpha} + q = 0, \tag{2}$$

$$N_{\alpha\beta,\beta} = 0, \tag{3}$$

where q is the load

$$M_{\alpha\beta} = \frac{1-\nu}{2} D \left(w_{\alpha,\beta} + w_{\beta,\alpha} + \frac{2\nu}{1-\nu} w_{\gamma,\gamma} \delta_{\alpha\beta} \right), \tag{4}$$

$$Q_\alpha = C(w_\alpha + w_{3,\alpha}), \tag{5}$$

$$N_{\alpha\beta} = N_{\alpha\beta}^{\text{linear}} + N_{\alpha\beta}^{\text{nonlinear}}, \tag{6}$$

$$N_{\alpha\beta}^{\text{linear}} = \frac{1-\nu}{2} B \left(u_{\alpha,\beta} + u_{\beta,\alpha} + \frac{2\nu}{1-\nu} u_{\gamma,\gamma} \delta_{\alpha\beta} \right), \tag{7}$$

$$N_{\alpha\beta}^{\text{nonlinear}} = \frac{1-\nu}{2} B \left(w_{3,\beta} w_{3,\alpha} + \frac{\nu}{1-\nu} w_{3,\gamma} w_{3,\gamma} \delta_{\alpha\beta} \right) . \tag{8}$$

Here $B(=Eh/\left(1-\nu^2\right))$ is the tension stiffness, $D(=Eh^3/\left[12\left(1-\nu^2\right)\right])$ is the bending stiffness of the plate, $C(=\left[D\,(1-\nu)\,\lambda^2\right]/2)$ is the shear stiffness, $\lambda(=\sqrt{10}/h)$ is the shear factor, h is the thickness of the plate, ν is Poisson's ratio, $N_{\alpha\beta}$ are in-plane stress resultants, Q_α and $M_{\alpha\beta}$ are out-of-plane stress resultants and moments, u_α and w_3 are translation of displacements in the x_1-, x_2-(in-plane) and x_3-(out-of-plane) directions, w_α are rotations in the x_α-direction, and $\delta_{\alpha\beta}$ is the Kronecker delta.

Indicial notation is used throughout this paper. Greek indices vary from 1 to 2, and Roman indices vary from 1 to 3.

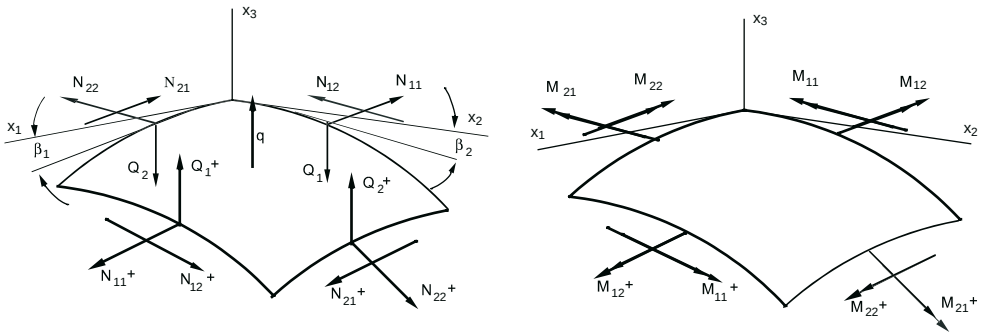

Figure 1. Stress resultant equilibrium for geometrically nonlinear plate element.

3. Boundary-integral equations

The derivation of boundary-integral equations for geometrically nonlinear plate-bending problems follows the linear analysis described by Dirgantara and Aliabadi [20] and Aliabadi [22]. Applying Betti's reciprocal theorem to the governing equations for the bending and transverse stress resultants at an arbitrary domain point $\mathbf{X}' \in \Omega$, we find

$$w_i(\mathbf{X}') + \int_\Gamma P^*_{ij}(\mathbf{X}', \mathbf{x}) w_j(\mathbf{x}) \mathrm{d}\Gamma(\mathbf{x}) = \int_\Gamma W^*_{ij}(\mathbf{X}', \mathbf{x}) p_j(\mathbf{x}) \mathrm{d}\Gamma(\mathbf{x}) + \\ + \int_\Omega W^*_{i3}(\mathbf{X}', \mathbf{X}) q(\mathbf{X}) \mathrm{d}\Omega(\mathbf{X}) + \int_\Omega W^*_{i3}(\mathbf{X}', \mathbf{X}) (N_{\alpha\beta} w_{3,\beta})_{,\alpha} \mathrm{d}\Omega(\mathbf{X}), \tag{9}$$

where Γ and Ω denote the boundary and domain respectively, $\mathbf{x}, \mathbf{x}' \in \Gamma$, $\mathbf{X}, \mathbf{X}' \in \Omega$ and

$$\{p\} = [M_{\alpha\beta} n_\beta, Q_\beta n_\beta].$$

In the same way, a boundary-integral equation for the in-plane displacements at domain point $\mathbf{X}'$ can be derived as

$$u_\theta(\mathbf{X}') + \int_\Gamma T^*_{\theta\alpha}(\mathbf{X}', \mathbf{x}) u_\alpha(\mathbf{x}) \mathrm{d}\Gamma(\mathbf{x}) = \int_\Gamma U^*_{\theta\alpha}(\mathbf{X}', \mathbf{x}) t^{\text{linear}}_\alpha(\mathbf{x}) \mathrm{d}\Gamma(\mathbf{x}) + \\ + \int_\Omega U^*_{\theta\alpha}(\mathbf{X}', \mathbf{X}) N^{\text{nonlinear}}_{\alpha\gamma,\gamma}(\mathbf{X}) \mathrm{d}\Omega(\mathbf{X}), \tag{10}$$

where

$$t^{\text{linear}}_\alpha = N^{\text{linear}}_{\alpha\beta} n_\beta.$$

Moving the point $\mathbf{X}'$ to the boundary, that is $\mathbf{X}' \to \mathbf{x}'$ at Γ, boundary-integral equations are obtained for the out-of-plane plate-bending problems

$$C_{ij} w_i(\mathbf{x}') + \int_\Gamma P^*_{ij}(\mathbf{x}', \mathbf{x}) w_j(\mathbf{x}) \mathrm{d}\Gamma(\mathbf{x}) = \int_\Gamma W^*_{ij}(\mathbf{x}', \mathbf{x}) p_j(\mathbf{x}) \mathrm{d}\Gamma(\mathbf{x}) + \\ + \int_\Omega W^*_{i3}(\mathbf{x}', \mathbf{X}) q(\mathbf{X}) \mathrm{d}\Omega(\mathbf{X}) + \int_\Omega W^*_{i3}(\mathbf{x}', \mathbf{X}) (N_{\alpha\beta} w_{3,\beta})_{,\alpha} \mathrm{d}\Omega(\mathbf{X}), \tag{11}$$

where $C_{ij} = \delta_{ij}/2$ for $\mathbf{x}'$ on a smooth boundary and

$$C_{\theta\alpha} u_\alpha(\mathbf{x}') + \int_\Gamma T^*_{\theta\alpha}(\mathbf{x}', \mathbf{x}) u_\alpha(\mathbf{x}) \mathrm{d}\Gamma(\mathbf{x}) = \int_\Gamma U^*_{\theta\alpha}(\mathbf{x}', \mathbf{x}) t^{\text{linear}}_\alpha(\mathbf{x}) \mathrm{d}\Gamma(\mathbf{x}) + \\ + \int_\Omega U^*_{\theta\alpha}(\mathbf{x}', \mathbf{X}) N^{\text{nonlinear}}_{\alpha\gamma,\gamma}(\mathbf{X}) \mathrm{d}\Omega(\mathbf{X}) \tag{12}$$

for the in-plane problems, where $C_{\theta\alpha}=\delta_{\theta\alpha}/2$ for $\mathbf{x}'$ on a smooth boundary. The fundamental solutions P^*_{ij}, $W^*_{ij,}$ $T^*_{\theta\alpha}$ and $U^*_{\theta\alpha}$ are listed in Appendix A.

4. Large-deformation analysis

In this section, two methods for evaluating the domain integrals that appear in the formulation are described: the domain-integral method and approximation-function method.

4.1. Domain-integral method

The nonlinear terms that appear in the domain integrals are calculated directly by use of a domain-integration procedure. Integrating by parts the last terms in Equations (11) and (12), we find

$$C_{ij}w_i(\mathbf{x}')+\int_\Gamma P^*_{ij}(\mathbf{x}',\mathbf{x})w_j(\mathbf{x})\mathrm{d}\Gamma(\mathbf{x})=\int_\Gamma W^*_{ij}(\mathbf{x}',\mathbf{x})p_j(\mathbf{x})\mathrm{d}\Gamma(\mathbf{x})+\int_\Omega W^*_{i3}(\mathbf{x}',\mathbf{X})q(\mathbf{X})\mathrm{d}\Omega(\mathbf{X})$$
$$+\int_\Gamma W^*_{i3}(\mathbf{x}',\mathbf{x})(N_{\alpha\beta}w_{3,\beta})\ n_\alpha(\mathbf{x})\mathrm{d}\Omega(\mathbf{X})-\int_\Omega W^*_{i3,\alpha}(\mathbf{x}',\mathbf{X})(N_{\alpha\beta}w_{3,\beta})\mathrm{d}\Omega(\mathbf{X}) \tag{13}$$

and

$$C_{\theta\alpha}u_\alpha(\mathbf{x}')+\int_\Gamma T^*_{\theta\alpha}(\mathbf{x}',\mathbf{x})u_\alpha(\mathbf{x})\mathrm{d}\Gamma(\mathbf{x})=\int_\Gamma U^*_{\theta\alpha}(\mathbf{x}',\mathbf{x})t^{\text{linear}}_\alpha(\mathbf{x})\mathrm{d}\Gamma(\mathbf{x})$$
$$=+\int_\Gamma U^*_{\theta\alpha}(\mathbf{x}',\mathbf{x})N^{\text{nonlinear}}_{\alpha\gamma}n_\gamma(\mathbf{x})\mathrm{d}\Gamma(\mathbf{X})-\int_\Omega U^*_{\theta\alpha,\gamma}(\mathbf{x}',\mathbf{X})N^{\text{nonlinear}}_{\alpha\gamma}(\mathbf{X})\mathrm{d}\Omega(\mathbf{X}), \tag{14}$$

which can be simplified to

$$C_{ij}w_i(\mathbf{x}')+\int_\Gamma P^*_{ij}(\mathbf{x}',\mathbf{x})w_j(\mathbf{x})\mathrm{d}\Gamma(\mathbf{x})=\int_\Gamma W^*_{ij}(\mathbf{x}',\mathbf{x})p_j(\mathbf{x})\mathrm{d}\Gamma(\mathbf{x})+$$
$$+\int_\Omega W^*_{i3}(\mathbf{x}',\mathbf{X})q(\mathbf{X})\mathrm{d}\Omega(\mathbf{X})-\int_\Omega W^*_{i3,\alpha}(\mathbf{x}',\mathbf{X})(N_{\alpha\beta}w_{3,\beta})\mathrm{d}\Omega(\mathbf{X}) \tag{15}$$

and

$$C_{\theta\alpha}u_\alpha(\mathbf{x}')+\int_\Gamma T^*_{\theta\alpha}(\mathbf{x}',\mathbf{x})u_\alpha(\mathbf{x})\mathrm{d}\Gamma(\mathbf{x})=\int_\Gamma U^*_{\theta\alpha}(\mathbf{x}',\mathbf{x})t_\alpha(\mathbf{x})\mathrm{d}\Gamma(\mathbf{x})-$$
$$-\int_\Omega U^*_{\theta\alpha,\gamma}(\mathbf{x}',\mathbf{X})N^{\text{nonlinear}}_{\alpha\gamma}(\mathbf{X})\mathrm{d}\Omega(\mathbf{X}), \tag{16}$$

where

$\{p\}=[M_{\alpha\beta}n_\beta,\ Q_\beta n_\beta]$ and $t_\alpha=N_{\alpha\beta}n_\beta$.

To calculate the nonlinear terms, two additional integral equations are required, including the derivative of deflection $w_{3,\gamma}$ equation

$$w_{3,\gamma}(\mathbf{X}')=\int_\Gamma W^*_{3j,\gamma}(\mathbf{X}',\mathbf{x})p_j(\mathbf{x})\mathrm{d}\Gamma(\mathbf{x})-\int_\Gamma P^*_{3j,\gamma}(\mathbf{X}',\mathbf{x})w_j(\mathbf{x})\mathrm{d}\Gamma(\mathbf{x})+$$
$$+\int_\Omega W^*_{33,\gamma}(\mathbf{X}',\mathbf{X})q(\mathbf{X})\mathrm{d}\Omega(\mathbf{X})-\int_\Omega W^*_{33,\gamma\alpha}(\mathbf{X}',\mathbf{X})(N_{\alpha\beta}w_{3,\beta})\ \mathrm{d}\Omega(\mathbf{X}) \tag{17}$$

and the membrane stress resultant $N^{\text{linear}}_{\alpha\beta}$ equation;

$$N^{\text{linear}}_{\alpha\beta}(\mathbf{X}')=\int_\Gamma U^*_{\delta\alpha\beta}(\mathbf{X}',\mathbf{x})t_\delta(\mathbf{x})\mathrm{d}\Gamma(\mathbf{x})-\int_\Gamma T^*_{\delta\alpha\beta}(\mathbf{X}',\mathbf{x})u_\delta(\mathbf{x})\mathrm{d}\Gamma(\mathbf{x})-$$
$$-\int_\Omega U^*_{\delta\alpha\beta}(\mathbf{X}',\mathbf{X})N^{\text{nonlinear}}_{\delta\gamma,\gamma}(\mathbf{X})\mathrm{d}\Omega(\mathbf{X}), \tag{18}$$

where the fundamental solutions $U^*_{\theta\alpha,\gamma}$, $W^*_{3j,\gamma}$, $W^*_{33,\gamma\alpha}$, $U^*_{\delta\alpha\beta}$, $T^*_{\delta\alpha\beta}$ and $U^*_{\delta\alpha\beta\gamma}$ are listed in Appendix A.

4.2. Approximation-function method and numerical implementation

An alternative formulation is now presented for dealing with the domain integrals due to the nonlinear terms. The main reason for this new formulation is to avoid direct calculation of the hypersingular integrals. Although the evaluation of these integrals is not extremely demanding with constant cells, higher-order cells require elaborate integration schemes (see [22]). The approximate-function method proposed here avoids these difficulties for higher-order cells. Equations (11) and (12) are used in this method. To calculate the nonlinear terms, three additional integral equations are required. The first equation is Equation (9), and the second equation is the derivative of deflection, $w_{3,\gamma}$ obtained from (9) as

$$w_{3,\gamma}(\mathbf{X}') = \int_\Gamma W^*_{3j,\gamma}(\mathbf{X}', \mathbf{x}) p_j(\mathbf{x}) \mathrm{d}\Gamma(\mathbf{x}) - \int_\Gamma P^*_{3j,\gamma}(\mathbf{X}', \mathbf{x}) w_j(\mathbf{x}) \mathrm{d}\Gamma(\mathbf{x}) + \\ + \int_\Omega W^*_{33,\gamma}(\mathbf{X}', \mathbf{X}) q(\mathbf{X}) \mathrm{d}\Omega(\mathbf{X}) + \int_\Omega W^*_{33,\gamma}(\mathbf{X}', \mathbf{X}) (N_{\alpha\beta} w_{3,\beta})_{,\alpha} \ \mathrm{d}\Omega(\mathbf{X}). \tag{19}$$

The third equation is the membrane stress resultant $N^{\text{linear}}_{\alpha\beta}$ representation obtained from (18) using (7):

$$N^{\text{linear}}_{\alpha\beta}(\mathbf{X}') = \int_\Gamma U^*_{\delta\alpha\beta}(\mathbf{X}', \mathbf{x}) t^{\text{linear}}_\delta(\mathbf{x}) \mathrm{d}\Gamma(\mathbf{x}) - \int_\Gamma T^*_{\delta\alpha\beta}(\mathbf{X}', \mathbf{x}) u_\delta(\mathbf{x}) \mathrm{d}\Gamma(\mathbf{x}) + \\ + \int_\Omega U^*_{\delta\alpha\beta}(\mathbf{X}', \mathbf{X}) N^{\text{nonlinear}}_{\delta\gamma,\gamma}(\mathbf{X}) \mathrm{d}\Omega(\mathbf{X}). \tag{20}$$

It can be seen that the nonlinear domain terms are now represented by $(N_{\alpha\beta} w_{3,\beta})_{,\alpha}$. The fundamental solution $W^*_{i3,\gamma}$ has a lower-order singularity than $W^*_{33,\gamma\alpha}$ appearing in Equation (17).

Equations (9), (11) and (19) can be rewritten in alternative forms

$$w_i(\mathbf{X}') + \int_\Gamma P^*_{ij}(\mathbf{X}', \mathbf{x}) w_j(\mathbf{x}) \mathrm{d}\Gamma(\mathbf{x}) = \int_\Gamma W^*_{ij}(\mathbf{X}', \mathbf{x}) p_j(\mathbf{x}) \mathrm{d}\Gamma(\mathbf{x}) + \\ + \int_\Omega W^*_{i3}(\mathbf{X}', \mathbf{X}) q(\mathbf{X}) \mathrm{d}\Omega(\mathbf{X}) + \int_\Omega W^*_{i3}(\mathbf{X}', \mathbf{X}) (N_{\alpha\beta,\alpha} w_{3,\beta} + N_{\alpha\beta} w_{3,\alpha\beta}) \mathrm{d}\Omega(\mathbf{X}), \tag{21}$$

$$C_{ij} w_i(\mathbf{x}') + \int_\Gamma P^*_{ij}(\mathbf{x}', \mathbf{x}) w_j(\mathbf{x}) \mathrm{d}\Gamma(\mathbf{x}) = \int_\Gamma W^*_{ij}(\mathbf{x}', \mathbf{x}) p_j(\mathbf{x}) \mathrm{d}\Gamma(\mathbf{x}) + \\ + \int_\Omega W^*_{i3}(\mathbf{x}', \mathbf{X}) q(\mathbf{X}) \mathrm{d}\Omega(\mathbf{X}) + \int_\Omega W^*_{i3}(\mathbf{x}', \mathbf{X}) (N_{\alpha\beta,\alpha} w_{3,\beta} + N_{\alpha\beta} w_{3,\alpha\beta}) \mathrm{d}\Omega(\mathbf{X}), \tag{22}$$

$$w_{3,\gamma}(\mathbf{X}') = \int_\Gamma W^*_{3j,\gamma}(\mathbf{X}', \mathbf{x}) p_j(\mathbf{x}) \mathrm{d}\Gamma(\mathbf{x}) - \int_\Gamma P^*_{3j,\gamma}(\mathbf{X}', \mathbf{x}) w_j(\mathbf{x}) \mathrm{d}\Gamma(\mathbf{x}) + \\ + \int_\Omega W^*_{33,\gamma}(\mathbf{X}', \mathbf{X}) q(\mathbf{X}) \mathrm{d}\Omega(\mathbf{X}) + \int_\Omega W^*_{33,\gamma}(\mathbf{X}', \mathbf{X}) (N_{\alpha\beta,\alpha} w_{3,\beta} + N_{\alpha\beta} w_{3,\alpha\beta}) \ \mathrm{d}\Omega(\mathbf{X}). \tag{23}$$

To calculate the derivatives of the nonlinear terms, the nonlinear terms are approximated by use of a radial basis function;

$$f^m(\mathbf{x}) = f(\mathbf{x}, \mathbf{x}^m) = \sqrt{C^2 + (r^m)^2}, \tag{24}$$

where $r^m(\mathbf{x}) = \sqrt{(x_1 - x_1^m)^2 + (x_2 - x_2^m)^2}$.

The nonlinear terms $N^{\text{nonlinear}}_{\delta\gamma,\gamma}$ in the in-plane Equations (12) and (20) are evaluated as:

$$N^{\text{nonlinear}}_{\delta\gamma}(x_1, x_2) = \sum_{m=1}^{M} f^m(\mathbf{X}) \Psi^m_{\delta\gamma}, \tag{25}$$

where M is the number of selected points, and the coefficients $\Psi_{\delta\gamma}^{m}$ are determined by values at the selected point m as

$$\boldsymbol{\Psi} = \mathbf{F}^{-1}\{N_{\delta\gamma}^{\text{nonlinear}}\}, \tag{26}$$

where $\mathbf{F} := f(x)$, $\{N_{\delta\gamma}^{\text{nonlinear}}\} := N_{\delta\alpha}^{\text{nonlinear}}(X^m)$; $m = 1, \ldots, M$ and

$$N_{\delta\gamma,\gamma}^{\text{nonlinear}}(x_1, x_2) = \mathbf{f}(\mathbf{X})_{,\gamma}\mathbf{F}^{-1}\{N_{\delta\gamma}^{\text{nonlinear}}\}. \tag{27}$$

Four approximations are available for calculating the nonlinear terms appearing in the plate-bending equation, as will be shown below.

4.2.1. *Approximation function method I*
The nonlinear terms $(N_{\alpha\beta}w_{3,\beta})_{,\alpha}$ in Equations (9), (11) and (19) are calculated as:

$$(N_{\alpha\beta}w_{3,\beta})(x_1, x_2) = \sum_{m=1}^{M} f^m(\mathbf{x})\Psi^m, \tag{28}$$

$$\boldsymbol{\Psi} = \mathbf{F}^{-1}\{N_{\alpha\beta}w_{3,\beta}\}, \tag{29}$$

$$(N_{\alpha\beta}w_{3,\beta})_{,\alpha}(x_1, x_2) = \mathbf{f}(\mathbf{x})_{,\alpha}\mathbf{F}^{-1}\{N_{\alpha\beta}w_{3,\beta}\}. \tag{30}$$

4.2.2. *Approximation function method II*
The nonlinear terms $(N_{\alpha\beta,\alpha}w_{3,\beta} + N_{\alpha\beta}w_{3,\alpha\beta})$ in Equations (21), (22) and (23) are calculated as follows.

For $N_{\alpha\beta,\alpha}$:

$$N_{\alpha\beta}(x_1, x_2) = \sum_{m=1}^{M} f^m(\mathbf{X})\Psi_{\alpha}^{m}, \tag{31}$$

$$\boldsymbol{\Psi} = \mathbf{F}^{-1}\{N_{\alpha\beta}\}, \tag{32}$$

where $\{N_{\alpha\beta}w_{3,\beta}\} = (N_{\alpha\beta}w_{3,\beta})(X^m)$, $m = 1, \ldots, M$

$$N_{\alpha\beta,\alpha}(x_1, x_2) = \mathbf{f}(\mathbf{X})_{,\alpha}\mathbf{F}^{-1}\{N_{\alpha\beta}\}. \tag{33}$$

For $w_{3,\alpha\beta}$:

$$w_{3,\beta}(x_1, x_2) = \sum_{m=1}^{M} f^m(\mathbf{X})\Psi_{\beta}^{m}, \tag{34}$$

$$\boldsymbol{\Psi} = \mathbf{F}^{-1}\{w_{3,\beta}\}, \tag{35}$$

where $\{w_{3,\beta}\} = w_{3,\beta}(X^m)$, $m = 1, \ldots M$,

$$w_{3,\alpha\beta}(x_1, x_2) = \mathbf{f}(\mathbf{X})_{,\alpha}\mathbf{F}^{-1}\{w_{3,\beta}\}. \tag{36}$$

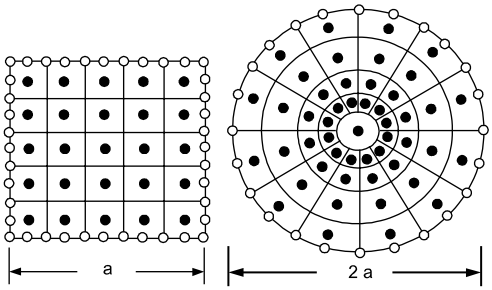

Figure 2. BEM model.

4.2.3. *Approximation function method III*
The term $N_{\alpha\beta,\alpha}$ is calculated in Equations (31)–(33). The terms $w_{3,\beta}$ and $w_{3,\alpha\beta}$ in Equations (21)–(23) are calculated as follows

$$w_3(x_1, x_2) = \sum_{m=1}^{M} f^m(\mathbf{X})\Psi^m, \tag{37}$$

$$\mathbf{\Psi} = \mathbf{F}^{-1}\{w_3\}, \tag{38}$$

where $\{w_3\} = w_3(X^m),\ m = 1, \ldots, M$

$$w_{3,\beta}(x_1, x_2) = \mathbf{f}(\mathbf{X})_{,\beta}\mathbf{F}^{-1}\{w_3\}, \tag{39}$$

$$w_{3,\alpha\beta}(x_1, x_2) = \mathbf{f}(\mathbf{X})_{,\alpha}\mathbf{f}(\mathbf{X})_{,\beta}\mathbf{F}^{-1}\{w_3\}. \tag{40}$$

4.2.4. *Approximation function method IV*
This approximation is the same as III, but involves selected points on the boundary and in the domain,

$$w_3(x_1, x_2) = \sum_{m=1}^{N+M} f^m(\mathbf{X})\Psi^m, \tag{41}$$

where N is a number of boundary nodes.

4.2.5. *Numerical implementation*
Quadratic isoparametric boundary elements were used to discretise the boundary, and constant cell elements (as shown in Figure 2) were used to descretize the domain. Details of the discretization procedures are given by [20].

5. Incremental approach and solution procedures

In this section, four methods are presented for dealing with the nonlinear problem.

5.1. Total incremental method

In this method, the load is divided into small load steps, and the equations are transformed into a system of algebraic equations,

$$[H^p]\{w^{k+1}\} + [G^p]\{p^{k+1}\} = [B^p]\{(N_{\alpha\beta}w_{3,\beta})^k_{,\alpha} + (k+1)\ \overset{\circ}{q}\}, \tag{42}$$

$$[H^m]\{u^{k+1}\}+[G^m]\{t^{k+1}\}=[B^m]\{N_{\alpha\beta,\beta}^{\text{nonlinear }(k)}\}, \tag{43}$$

where k denotes the incremental step; the superscript $\overset{\circ}{(.)}$ denotes the incremental value of a term.

Once the matrices $[H^p]$, $[G^p]$, $[B^p]$, $[H^m]$, $[G^m]$ and $[B^m]$ have been formed, they can be stored and used in each increment without any further change. Moreover, the system of equations can be solved by the LU-decomposition method, slightly modified to store the matrix coefficients in the core and reuse in each increment.

In the loading step, the $(k+1)^{\text{th}}$ approximation is estimated by use of the kth approximation for the terms on the right-hand side. Suppose that $\overset{\circ}{N}_{\alpha\beta}{}^{(k)}$ and $\overset{\circ}{w}_{3,\beta}{}^{(k)}$ express the k^{th} approximations. The initial values of the first loading step $(k=1)$ can be set, for example $\overset{\circ}{N}_{\alpha\beta}{}^{\text{linear}(k)}=0$, and $\overset{\circ}{w}_{3,\beta}{}^{(k)}=0$. The loading step in each increment, $q=(k+1)\ \overset{\circ}{q}$.

Relaxation procedures are adopted to improve the numerical results. When the nonlinear terms are calculated in each step of increment, the deflection w_3, and its derivative $w_{3,\beta}$, can be modified as follows:

$$\hat{w}_3^{k+1}=\varepsilon\ w_3^{k+1}+(1-\varepsilon)\ w_3^k, \tag{44}$$

$$\hat{w}_{3,\beta}^{k+1}=\varepsilon\ w_{3,\beta}^{k+1}+(1-\varepsilon)\ w_{3,\beta}^k, \tag{45}$$

where ε is chosen as 0·5 and $k\geq 2$. The flow chart of the total increment method is shown in Figure 3.

5.2. Cumulative load incremental method

Alternatively, the total load could be presented as a cumulative load incremental method. The nonlinear tensors $\overset{\circ}{N}_{\alpha\beta}{}^{\text{nonlinear}}$ are written as

$$\overset{\circ}{N}_{11}^{\text{nonlinear}(k)}=\frac{B}{2}\left[2w_{3,1}^{k-1}\,\overset{\circ}{w}_{3,1}^{k}+\overset{\circ}{w}_{3,1}^{k}\overset{\circ}{w}_{3,1}^{k}+\nu(2w_{3,2}^{k-1}\,\overset{\circ}{w}_{3,2}^{k}+\overset{\circ}{w}_{3,2}^{k}\overset{\circ}{w}_{3,2}^{k})\right], \tag{46}$$

$$\overset{\circ}{N}_{22}^{\text{nonlinear}(k)}=\frac{B}{2}\left[2w_{3,2}^{k-1}\,\overset{\circ}{w}_{3,2}^{k}+\overset{\circ}{w}_{3,2}^{k}\overset{\circ}{w}_{3,2}^{k}+\nu(2w_{3,1}^{k-1}\,\overset{\circ}{w}_{3,1}^{k}+\overset{\circ}{w}_{3,1}^{k}\overset{\circ}{w}_{3,1}^{k})\right], \tag{47}$$

$$\overset{\circ}{N}_{12}^{\text{nonlinear}(k)}=\frac{1-\nu}{2}B\left[w_{3,1}^{k-1}\,\overset{\circ}{w}_{3,2}^{k}+\overset{\circ}{w}_{3,1}^{k}\overset{\circ}{w}_{3,2}^{k}+w_{3,2}^{k-1}\,\overset{\circ}{w}_{3,1}^{k}\right]. \tag{48}$$

The equations can be written in terms of the incremental values. The loads are divided into small load steps, and the equations are represented as an incremental system of algebraic equations:

$$[H^p]\left\{\overset{\circ}{w}^{k+1}\right\}+[G^p]\left\{\overset{\circ}{p}^{k+1}\right\}=[B^p]\left\{\left(\overset{o}{N}_{\alpha\beta}\overset{\circ}{w}_{3,\beta}\right)_{,\alpha}^{k}+\overset{\circ}{q}\right\}, \tag{49}$$

$$[H^m]\left\{\overset{\circ}{u}^{k+1}\right\}+[G^m]\left\{\overset{\circ}{t}^{\,k+1}\right\}=[B^m]\left\{\overset{o}{N}_{\alpha\beta,\beta}^{\text{nonlinear}(k)}\right\}, \tag{50}$$

where k denotes incremental step; superscript $\overset{\circ}{(.)}$ is incremental of term.

Similar to the total incremental method, once the matrices $[H^p]$, $[G^p]$, $[B^p]$, $[H^m]$, $[G^m]$ and $[B^m]$ have been calculated, they can be used in each increment step. The loading is done

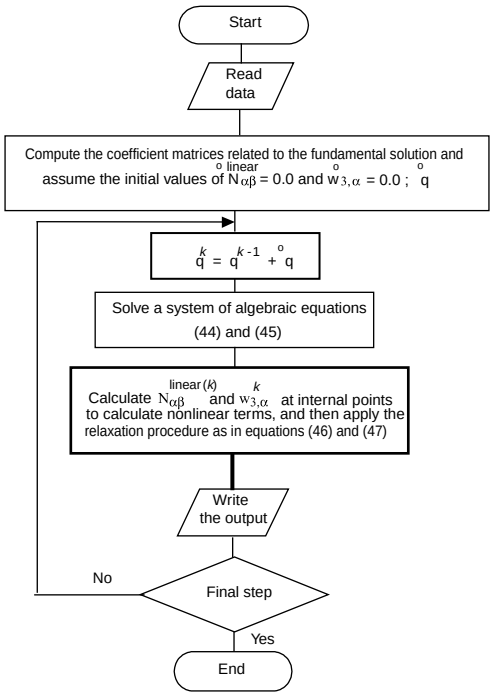

Figure 3. Flow chart of the total incremental method.

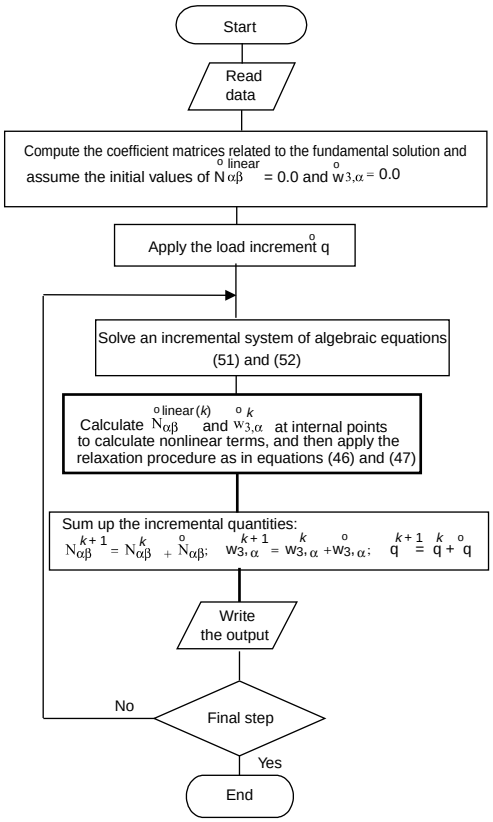

Figure 4. Flow chart of sub-incremental cumulative method.

in small constant loading step $\overset{\circ}{q}$. Then the incremental quantities obtained at each loading step are simply summed up and the modified LU-decomposition is used to solve the system of equations. The relaxation procedures as described in Equations (44) and (45) are applied. The flow chart of the sub-incremental cumulative method is shown in Figure 4.

5.3. Euler method

The Euler method is similar to the cumulative load incremental method, but the terms $\overset{\circ}{N}{}^{\text{nonlinear}}_{\alpha\beta}$ are expressed as the first derivative of N_{α_β};

$$\overset{\circ}{N}{}^{\text{nonlinear}(k)}_{11} = B\left(w^{k}_{3,1}\,\overset{\circ}{w}{}^{k}_{3,1} + \nu w^{k}_{3,2}\,\overset{\circ}{w}{}^{k}_{3,2}\right), \tag{51}$$

$$\overset{\circ}{N}{}^{\text{nonlinear}(k)}_{22} = B\left(w^{k}_{3,2}\,\overset{\circ}{w}{}^{k}_{3,2} + \nu w^{k}_{3,1}\,\overset{\circ}{w}{}^{k}_{3,1}\right), \tag{52}$$

$$\overset{\circ}{N}{}^{\text{nonlinear}(k)}_{12} = \frac{1-\nu}{2} B\left(w^{k}_{3,1}\,\overset{\circ}{w}{}^{k}_{3,2} + w^{k}_{3,2}\,\overset{\circ}{w}{}^{k}_{3,1}\right), \tag{53}$$

where $w_{3,\alpha}^{k+1} = w_{3,\alpha}^{k} + \overset{\circ}{w}{}_{3,\alpha}^{k}$. Therefore the system of algebraic equations can be written as follows:

$$[B]\left\{ \overset{\circ}{w}{}^{k+1} \right\} + [C]\left\{ \overset{\circ}{p}{}^{k+1} \right\} = [D]\left\{ \left(N_{\alpha\beta}^{k} \overset{\circ}{w}{}_{3,\alpha}^{k} + \overset{\circ}{N}{}_{\alpha\beta}^{k} w_{3,\beta}^{k} \right)_{,\alpha} + \overset{\circ}{q} \right\}, \tag{54}$$

$$[E]\left\{ \overset{\circ}{u}{}^{k+1} \right\} + [F]\left\{ \overset{\circ}{t}{}^{k+1} \right\} = [G]\left\{ \overset{\circ}{N}{}_{\alpha\beta,\beta}^{\text{nonlinear}(k)} \right\}, \tag{55}$$

where $N_{\alpha\beta}^{k+1} = N_{\alpha\beta}^{k} + \overset{\circ}{N}{}_{\alpha\beta}^{k}$. The loading is also provided in a small loading step $\overset{\circ}{q}$. The previous incremental quantities obtained are simply summed up in each loading step. The modified LU-decomposition is also adopted to solve the system of equations. The relaxation procedures as described for Equations (44) and (45) are applied. The flow chart of the Euler method is similar to the flow chart for sub-incremental cumulative method.

5.4. Nonlinear-system method

This method can only be applied to the domain-integral method. By introducing the increment terms into the Equations (15)–(18), such that $w_i^{k+1} = w_i^k + \overset{\circ}{w}_i$; $u_\alpha^{k+1} = u_\alpha^k + \overset{\circ}{u}_\alpha$; *etc;* the boundary-integral equations for plate bending can be rewritten as

$$\begin{aligned} &C_{ij}(w_i^k(\mathbf{x}') + \overset{\circ}{w}_i(\mathbf{x}')) + \int_\Gamma P_{ij}^*(\mathbf{x}', \mathbf{x})(w_j^k(\mathbf{x}) + \overset{\circ}{w}_j(\mathbf{x}))\mathrm{d}\Gamma(\mathbf{x}) = \\ &= \int_\Gamma W_{ij}^*(\mathbf{x}', \mathbf{x})(p_j^k(\mathbf{x}) + \overset{\circ}{p}_j(\mathbf{x}))\mathrm{d}\Gamma(\mathbf{x}) + \int_\Omega W_{i3}^*(\mathbf{x}', \mathbf{X})(q^k(\mathbf{X}) + \overset{\circ}{q}(\mathbf{X}))\mathrm{d}\Omega(\mathbf{X}) - \\ &\quad - \int_\Omega W_{i3,\alpha}^*(\mathbf{x}', \mathbf{X})((N_{\alpha\beta}^k + \overset{\circ}{N}_{\alpha\beta})(w_{3,\beta}^k + \overset{\circ}{w}_{3,\beta}))\mathrm{d}\Omega(\mathbf{X}). \end{aligned} \tag{56}$$

Neglecting the higher-order incremental terms, we have

$$\begin{aligned} &C_{ij}(w_i^k(\mathbf{x}') + \overset{\circ}{w}_i(\mathbf{x}')) + \int_\Gamma P_{ij}^*(\mathbf{x}', \mathbf{x})(w_j^k(\mathbf{x}) + \overset{\circ}{w}_j(\mathbf{x}))\mathrm{d}\Gamma(\mathbf{x}) = \\ &= \int_\Gamma W_{ij}^*(\mathbf{x}', \mathbf{x})(p_j^k(\mathbf{x}) + \overset{\circ}{p}_j(\mathbf{x}))\mathrm{d}\Gamma(\mathbf{x}) + \int_\Omega W_{i3}^*(\mathbf{x}', \mathbf{X})(q^k(\mathbf{X}) + \overset{\circ}{q}(\mathbf{X}))\mathrm{d}\Omega(\mathbf{X}) - \\ &\quad - \int_\Omega W_{i3}^*(\mathbf{x}', \mathbf{X})((N_{\alpha\beta}^k w_{3,\beta}^k + N_{\alpha\beta}^k \overset{\circ}{w}_{3,\beta}))\mathrm{d}\Omega(\mathbf{X}) - \\ &\quad - \int_\Omega W_{i3,\alpha}^*(\mathbf{x}', \mathbf{X})((\frac{1-\nu}{2} B(w_{3,\beta}^k \overset{\circ}{w}_{3,\alpha} + \overset{\circ}{w}_{3,\beta} w_{3,\alpha}^k + 2\frac{\nu}{1-\nu} w_{3,\gamma}^k \overset{\circ}{w}_{3,\gamma} \delta_{\alpha\beta}))w_{3,\beta}^k)\mathrm{d}\Omega(\mathbf{X}) - \\ &\quad - \int_\Omega W_{i3,\alpha}^*(\mathbf{x}', \mathbf{X})(\overset{\circ}{N}{}_{\alpha\beta}^{\text{linear}} w_{3,\beta}^k)\mathrm{d}\Omega(\mathbf{X}). \end{aligned} \tag{57}$$

The boundary-integral equations for the membrane are:

$$\begin{aligned} &C_{\theta\alpha}(u_\alpha^k(\mathbf{x}') + \overset{\circ}{u}_\alpha(\mathbf{x}')) + \int_\Gamma T_{\theta\alpha}^*(\mathbf{x}', \mathbf{x})(u_\alpha^k(\mathbf{x}) + \overset{\circ}{u}_\alpha(\mathbf{x}))\mathrm{d}\Gamma(\mathbf{x}) = \\ &= \int_\Gamma U_{\theta\alpha}^*(\mathbf{x}', \mathbf{x})(t_\alpha^k(\mathbf{x}) + \overset{\circ}{t}_\alpha(\mathbf{x}))\mathrm{d}\Gamma(\mathbf{x}) - \int_\Omega U_{\theta\alpha,\gamma}^*(\mathbf{x}', \mathbf{X}) N_{\alpha\gamma}^{\text{nonlinear } k}(\mathbf{X})\mathrm{d}\Omega(\mathbf{X}) - \\ &\quad - \int_\Omega U_{\theta\alpha,\gamma}^*(\mathbf{x}', \mathbf{X})(\frac{1-\nu}{2} B(w_{3,\alpha}^k \overset{\circ}{w}_{3,\gamma} + \overset{\circ}{w}_{3,\alpha} w_{3,\gamma}^k + 2\frac{\nu}{1-\nu} w_{3,\eta}^k \overset{\circ}{w}_{3,\eta} \delta_{\alpha\beta})\mathrm{d}\Omega(\mathbf{X}). \end{aligned} \tag{58}$$

The derivative of the out-of-plane displacement is described by

$$
\begin{aligned}
&w^k_{3,\gamma}(\mathbf{X}')+\overset{\circ}{w}_{3,\gamma}(\mathbf{X}')=\int_\Gamma W^*_{3j,\gamma}(\mathbf{X}',\mathbf{x})(p^k_j(\mathbf{x})+\overset{\circ}{p}_j(\mathbf{x}))\mathrm{d}\Gamma(\mathbf{x})-\\
&-\int_\Gamma P^*_{3j,\gamma}(\mathbf{X}',\mathbf{x})(w^k_j(\mathbf{x})+\overset{\circ}{w}_j(\mathbf{x}))\mathrm{d}\Gamma(\mathbf{x})+\int_\Omega W^*_{33,\gamma}(\mathbf{X}',\mathbf{X})(q^k(\mathbf{X})+\overset{\circ}{q}(\mathbf{X}))\mathrm{d}\Omega(\mathbf{X})-\\
&-\int_\Omega W^*_{33,\gamma\alpha}(\mathbf{X}',\mathbf{X})((N^k_{\alpha\beta}w^k_{3,\beta}+N^k_{\alpha\beta}\overset{\circ}{w}_{3,\beta}))\ \mathrm{d}\Omega(\mathbf{X})-\\
&-\int_\Omega W^*_{33,\gamma\alpha}(\mathbf{X}',\mathbf{X})(\frac{1-\nu}{2}B(w^k_{3,\beta}\overset{\circ}{w}_{3,\alpha}+\overset{\circ}{w}_{3,\beta}w^k_{3,\alpha}+\\
&+2\frac{\nu}{1-\nu}w^k_{3,\gamma}\overset{\circ}{w}_{3,\gamma}\delta_{\alpha\beta})w^k_{3,\beta})\mathrm{d}\Omega(\mathbf{X})+\int_\Omega W^*_{33,\gamma\alpha}(\mathbf{X}',\mathbf{X})(\overset{\circ}{N}{}^{\text{linear}}_{\alpha\beta}w^k_{3,\beta})\mathrm{d}\Omega(\mathbf{X}).
\end{aligned}
\tag{59}
$$

The membrane stress resultants are described by

$$
\begin{aligned}
&N^{\text{linear }k}_{\alpha\beta}(\mathbf{X}')+\overset{\circ}{N}{}^{\text{linear}}_{\alpha\beta}(\mathbf{X}')=\int_\Gamma U^*_{\Delta\alpha\beta}(\mathbf{X}',\mathbf{x})(t^k_\Delta(\mathbf{x})+\overset{\circ}{t}_\Delta(\mathbf{x}))\mathrm{d}\Gamma(\mathbf{x})-\\
&-\int_\Gamma T^*_{\Delta\alpha\beta}(\mathbf{X}',\mathbf{x})(u^k_\Delta(\mathbf{x})+\overset{\circ}{u}_\Delta(\mathbf{x}))\mathrm{d}\Gamma(\mathbf{x})-\int_\Omega U^*_{\Delta\alpha\beta,\gamma}(\mathbf{X}',\mathbf{X})N^{\text{nonlinear }k}_{\Delta\gamma}(\mathbf{X})\mathrm{d}\Omega(\mathbf{X})-\\
&-\int_\Omega U^*_{\Delta\alpha\beta,\gamma}(\mathbf{X}',\mathbf{X})(\frac{1-\nu}{2}B(w^k_{3,\Delta}\overset{\circ}{w}_{3,\gamma}+\overset{\circ}{w}_{3,\Delta}w^k_{3,\gamma}+2\frac{\nu}{1-\nu}w^k_{3,\eta}\overset{\circ}{w}_{3,\eta}\delta_{\alpha\beta})\mathrm{d}\Omega(\mathbf{X}).
\end{aligned}
\tag{60}
$$

Rearranging Equations (57)–(60), so that all unknown incremental terms are on the left-hand side, we obtain

$$
\begin{aligned}
&C_{ij}\overset{\circ}{w}_i(\mathbf{x}')+\int_\Gamma P^*_{ij}(\mathbf{x}',\mathbf{x})\overset{\circ}{w}_j(\mathbf{x})\mathrm{d}\Gamma(\mathbf{x})-\int_\Gamma W^*_{ij}(\mathbf{x}',\mathbf{x})\overset{\circ}{p}_j(\mathbf{x})\mathrm{d}\Gamma(\mathbf{x})+\\
&\quad+\int_\Omega W^*_{i3,\alpha}(\mathbf{x}',\mathbf{X})(N^k_{\alpha\beta}\overset{\circ}{w}_{3,\beta})\mathrm{d}\Omega(\mathbf{X})+\int_\Omega W^*_{i3,\alpha}(\mathbf{x}',\mathbf{X})(w^k_{3,\beta}(\frac{1-\nu}{2}B(\overset{\circ}{w}{}^k_{3,\beta}\overset{\circ}{w}_{3,\alpha}+\\
&\quad+\overset{\circ}{w}_{3,\beta}w^k_{3,\alpha}+2\frac{\nu}{1-\nu}w_{3,\gamma}\overset{\circ}{w}_{3,\gamma}\delta_{\alpha\beta})))\mathrm{d}\Omega(\mathbf{X})+\int_\Omega W^*_{i3,\alpha}(\mathbf{x}',\mathbf{X})(w^k_{3,\beta}\overset{\circ}{N}{}^{\text{linear}}_{\alpha\beta})\mathrm{d}\Omega(\mathbf{X})=\\
&=\int_\Omega W^*_{i3}(\mathbf{x}',\mathbf{X})(q^k(\mathbf{X})+\overset{\circ}{q}(\mathbf{X}))\mathrm{d}\Omega(\mathbf{X})-C_{ij}w^k_i(\mathbf{x}')+\int_\Gamma W^*_{ij}(\mathbf{x}',\mathbf{x})p^k_j(\mathbf{x})\mathrm{d}\Gamma(\mathbf{x})+\\
&\quad-\int_\Omega W^*_{i3}(\mathbf{x}',\mathbf{X})(N^k_{\alpha\beta}w^k_{3,\beta})\mathrm{d}\Omega(\mathbf{X})-\int_\Gamma P^*_{ij}(\mathbf{x}',\mathbf{x})w^k_j(\mathbf{x})\mathrm{d}\Gamma(\mathbf{x})
\end{aligned}
\tag{61}
$$

for plate bending problems,

$$
\begin{aligned}
&C_{\theta\alpha}\overset{\circ}{u}_\alpha(\mathbf{x}')+\int_\Gamma T^*_{\theta\alpha}(\mathbf{x}',\mathbf{x})\overset{\circ}{u}_\alpha(\mathbf{x})\mathrm{d}\Gamma(\mathbf{x})-\int_\Gamma U^*_{\theta\alpha}(\mathbf{x}',\mathbf{x})\overset{\circ}{t}_\alpha(\mathbf{x})\mathrm{d}\Gamma(\mathbf{x})+\\
&\quad+\int_\Omega U^*_{\theta\alpha,\gamma}(\mathbf{x}',\mathbf{X})(\frac{1-\nu}{2}B(w^k_{3,\alpha}\overset{\circ}{w}_{3,\gamma}+\overset{\circ}{w}_{3,\alpha}w^k_{3,\gamma}+2\frac{\nu}{1-\nu}w^k_{3,\eta}\overset{\circ}{w}_{3,\eta}\delta_{\alpha\beta})\mathrm{d}\Omega(\mathbf{X})=\\
&=\int_\Gamma U^*_{\theta\alpha}(\mathbf{x}',\mathbf{x})t^k_\alpha(\mathbf{x})\mathrm{d}\Gamma(\mathbf{x})-C_{\theta\alpha}u^k_\alpha(\mathbf{x}')-\int_\Omega U^*_{\theta\alpha,\gamma}(\mathbf{x}',\mathbf{X})N^{\text{nonlinear }k}_{\alpha\gamma}(\mathbf{X})\mathrm{d}\Omega(\mathbf{X})-\\
&\quad-\int_\Gamma T^*_{\theta\alpha}(\mathbf{x}',\mathbf{x})u^k_\alpha(\mathbf{x})\mathrm{d}\Gamma(\mathbf{x})
\end{aligned}
\tag{62}
$$

for membrane problems,

$$\begin{aligned}
&\overset{\circ}{w}_{3,\gamma}(\mathbf{X}') - \int_\Gamma W^*_{3j,\gamma}(\mathbf{X}',\mathbf{x})\,\overset{\circ}{p}_j(\mathbf{x})\mathrm{d}\Gamma(\mathbf{x}) + \int_\Gamma P^*_{3j,\gamma}(\mathbf{X}',\mathbf{x})\,\overset{\circ}{w}_j(\mathbf{x})\mathrm{d}\Gamma(\mathbf{x}) - \\
&\quad - \int_\Omega W^*_{33,\gamma\alpha}(\mathbf{X}',\mathbf{X})(w^k_{3,\beta}(\frac{1-\nu}{2}B(w^k_{3,\beta}\,\overset{\circ}{w}_{3,\alpha} + \overset{\circ}{w}_{3,\beta}\,w^k_{3,\alpha} + \\
&\quad + 2\frac{\nu}{1-\nu}w^k_{3,\gamma}\,\overset{\circ}{w}_{3,\gamma}\,\delta_{\alpha\beta}))\mathrm{d}\Omega(\mathbf{X}) - \int_\Omega W^*_{33,\gamma\alpha}(\mathbf{X}',\mathbf{X})(N^k_{\alpha\beta}\,\overset{\circ}{w}_{3,\beta})\ \mathrm{d}\Omega(\mathbf{X}) - \\
&\quad - \int_\Omega W^*_{33,\gamma\alpha}(\mathbf{X}',\mathbf{X})(\overset{\circ}{N}{}^{\text{linear}}_{\alpha\beta}\ w^k_{3,\beta})\mathrm{d}\Omega(\mathbf{X}) = \int_\Gamma W^*_{3j,\gamma}(\mathbf{X}',\mathbf{x})\,p^k_j(\mathbf{x})\mathrm{d}\Gamma(\mathbf{x}) - w^k_{3,\gamma}(\mathbf{X}') - \\
&\quad - \int_\Omega W^*_{33,\gamma\alpha}(\mathbf{X}',\mathbf{X})(N^k_{\alpha\beta}w^k_{3,\beta})\ \mathrm{d}\Omega(\mathbf{X}) + \int_\Omega W^*_{33,\gamma}(\mathbf{X}',\mathbf{X})(q^k(\mathbf{X}) + \overset{\circ}{q}(\mathbf{X}))\mathrm{d}\Omega(\mathbf{X}) - \\
&\quad - \int_\Gamma P^*_{3j,\gamma}(\mathbf{X}',\mathbf{x})w^k_j(\mathbf{x})\mathrm{d}\Gamma(\mathbf{x})
\end{aligned} \tag{63}$$

for the derivative of deflection, and

$$\begin{aligned}
&\overset{\circ}{N}{}^{\text{linear}}_{\alpha\beta}(\mathbf{X}') - \int_\Gamma U^*_{\Delta\alpha\beta}(\mathbf{X}',\mathbf{x})\,\overset{\circ}{t}_\Delta(\mathbf{x})\mathrm{d}\Gamma(\mathbf{x}) + \int_\Gamma T^*_{\Delta\alpha\beta}(\mathbf{X}',\mathbf{x})\,\overset{\circ}{u}_\Delta(\mathbf{x})\mathrm{d}\Gamma(\mathbf{x}) + \\
&\quad + \int_\Omega U^*_{\Delta\alpha\beta,\gamma}(\mathbf{X}',\mathbf{X})(\frac{1-\nu}{2}B(w_{3,\Delta}\,\overset{\circ}{w}_{3,\gamma} + \overset{\circ}{w}_{3,\Delta}\,w_{3,\gamma} + 2\frac{\nu}{1-\nu}w_{3,\eta}\,\overset{\circ}{w}_{3,\eta}\,\delta_{\alpha\beta})\mathrm{d}\Omega(\mathbf{X}) = \\
&= \int_\Gamma U^*_{\Delta\alpha\beta}(\mathbf{X}',\mathbf{x})t^k_\Delta(\mathbf{x})\mathrm{d}\Gamma(\mathbf{x}) - N^{\text{linear}}_{\alpha\beta}(\mathbf{X}') - \int_\Gamma T^*_{\Delta\alpha\beta}(\mathbf{X}',\mathbf{x})u^k_\Delta(\mathbf{x})\mathrm{d}\Gamma(\mathbf{x}) - \\
&\quad - \int_\Omega U^*_{\Delta\alpha\beta,\gamma}(\mathbf{X}',\mathbf{X})N^{\text{nonlinear}}_{\Delta\gamma}(k)(\mathbf{X})\mathrm{d}\Omega(\mathbf{X})
\end{aligned} \tag{64}$$

for the linear membrane stress resultants.

It can be seen that there are ten unknown incremental variables $\overset{\circ}{p}(\mathbf{x})$, $\overset{\circ}{w}(\mathbf{x})$, $\overset{\circ}{t}(\mathbf{x})$ and $\overset{\circ}{u}(\mathbf{x})$ on the boundary, and five variables $\overset{\circ}{N}{}^{\text{linear}}_{\alpha\beta}$, $\overset{\circ}{w}_{3,\Delta}$ in the domain. Equations (61)–(64) can be collected into the following final system of equations:

$$A\ \Delta\mathbf{X} = \Delta F. \tag{65}$$

In this case, the matrix A is updated in each load increment.

For an iteration process, the Newton-Raphson procedure is adopted together with the Equations (61)–(64). The matrix A is updated in each iteration. The iteration calculation is repeated until the following convergence condition for the k^{th} iteration and the $(k+1)^{\text{th}}$ iteration is satisfied,

$$\left|\frac{w^{k+1}_{\max} - w^k_{\max}}{w^k_{\max}}\right| \le \varepsilon \tag{66}$$

where ε is a small convergence parameter. The flow chart of the simultaneous integral method is shown in Figure 5.

6. Numerical examples

To assess the accuracy of the proposed methods for the analysis of problems involving large deformations, several examples with two restraint models and combination of them are presented in Figure 6. The BEM models for domain cell integration are shown in Figure 2.

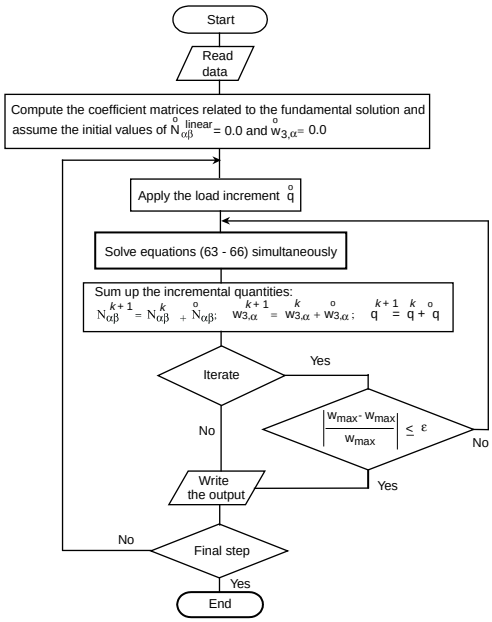

Figure 5. Flow chart of the nonlinear system of equation method.

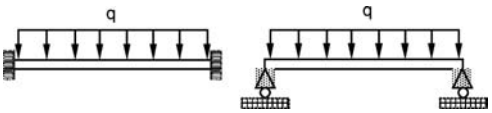

Figure 6. Restraint models.

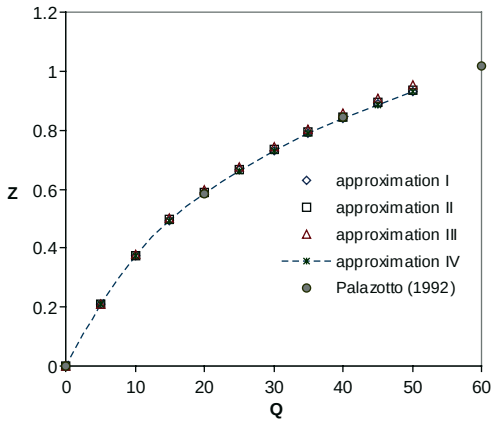

Figure 7. Simply supported square plate subjected to uniform transverse loads q computed with the domain integrals treated using the domain-cell technique.

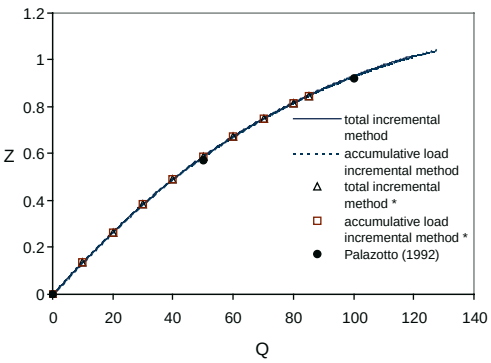

Figure 8. Comparison of total increment method and sub increment method. (*) without relaxation.

Comparisons are made with other numerical methods and analytical results. In the following examples, the dimensionless parameters are defined as follows:

$$Q = \frac{q\ a^4}{E\ h^4}\ , \tag{67}$$

$$Z = \frac{w_3^{\max}}{h}, \tag{68}$$

where a is the radius of a circular plate or width of a square plate, h is the plate thickness, q is the uniformly lateral distributed load, E is the modulus of elasticity, and w_3 is the lateral deflection. The following abbreviations are used:

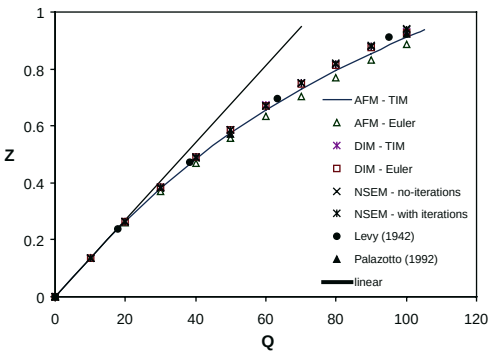

Figure 9. Clamped square plate subjected to a uniform load, q.

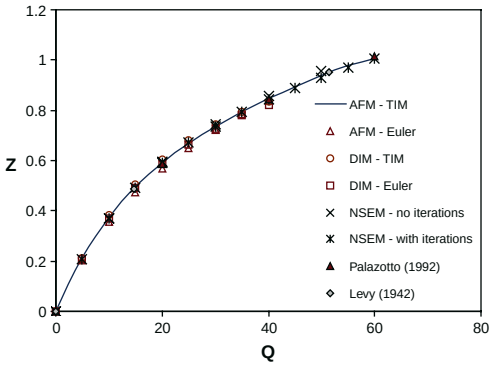

Figure 10. Simply supported square plate subjected to a uniform load, q.

AFM: approximation-function method (domain cells), DIM: domain-integral method (domain cells), for domain-integral evaluations. TIM: total-increment method, Euler: Euler method, NSEM: nonlinear system of equations method, for solution procedures.

6.1. Study of different approximation functions

This example is used to study the accuracy of the different approximation-function methods proposed for large deformation analysis. Four different approximations as described in Section 4.2 are used to evaluate the nonlinear terms which appear in the plate-bending equation. A simply supported square plate subjected to uniform transverse loads is considered. Assuming that the center of plate is at the origin, we obtain the boundary condition for this case as follows:

$$\text{Along } x = \pm a/2: \qquad u_1 = u_2 = w_3 = 0, \quad M_{12} = M_{11} = 0$$
$$\text{Along } y = \pm a/2: \qquad u_1 = u_2 = w_3 = 0, \quad M_{12} = M_{22} = 0$$

BEM meshes with 20 quadratic boundary-elements, and 25 domain cells (for domain integration) are used. The normalized maximum deflection values Z are plotted in Figure 7 and compared with finite-element results [23]. It can be seen from the Figure 7 that the results of all approximations are in good agreement (less than 1·5% difference) with the finite-element results.

6.2. Total incremental method *vs.* cumulative-load incremental method

In this example, the accuracy and efficiency of the total increment method and the sub-increment method are compared. A comparison is also made of both methods with the implementation of the relaxation procedure described in Section 5.1. In this case study, a clamped square plate subjected to a uniform transverse load q is analyzed. If the origin point (0·0,0·0) is located at the center of plate, then the boundary conditions are:

$$\text{Along } x = \pm a/2: \qquad u_1 = u_2 = w_1 = w_2 = w_3 = 0$$
$$\text{Along } y = \pm a/2: \qquad u_1 = u_2 = w_1 = w_2 = w_3 = 0$$

BEM meshes with 20 quadratic boundary elements and 25 domain cells are used in this analysis. The normalized maximum deflection values $\underline{w}$ are plotted in Figure 8 and compared with finite-element results [23]. It can be seen from Figure 8, that the cumulative-load incremental method is identical with the total incremental method. The results of both methods are in good agreement with the reference results. By introducing the relaxation procedure, we

can improve the numerical results. Without the relaxation procedure, the increment process may involve fewer increments.

6.3. Clamped square plate

In this example, a plate is subjected to a uniform distribution load q (see Figures 2 and 6). Considering the origin point (0·0,0·0) as the center of the plate, we have the following boundary conditions for this case:

$$\text{Along } x = \pm a/2: \qquad u_1 = u_2 = w_1 = w_2 = w_3 = 0,$$
$$\text{Along } y = \pm a/2: \qquad u_1 = u_2 = w_1 = w_2 = w_3 = 0.$$

BEM meshes with 20 quadratic boundary elements and 25 domain cells are used. The problem is analyzed with different solution procedures, *i.e.,* total increment method, the Euler method and the simultaneous integral method with and without iterations. The normalized maximum deflection values Z are plotted in Figure 9.

The results are compared with the finite-element result [23] and the analytical result [2]. Most BEM results differ less than 3% from the reference values but the results obtained using the approximation-function method with a solution procedure involving the Euler method exhibit larger errors for increasing values of Q.

6.4. Simply supported square plate

Here a simply supported plate subjected to a uniform distribution load q (see Figures 2 and 6) is analyzed. The boundary conditions are: $u_1 = u_2 = w_3 = 0$, $M_{\alpha\beta} n_\beta = 0$ along all sides.

BEM meshes with 20 quadratic boundary elements and 25 domain cells are used. The problem is analyzed with different solution procedures, *i.e.,* total increment method, Euler method and simultaneous integral method with and without iterations. The normalized maximum deflection values Z are plotted in Figure 10. The normalized BEM values of maximum deflection of the plate, finite-element result [23] and the analytical result [2] are plotted in Figure 10. Good agreement with the references ($< 2\%$ difference) is achieved.

6.5. A square plate with clamped and simply supported edges

A plate subjected to a uniform transverse load q (see Figure 2 and Figure 6) is analyzed. The boundary conditions for this case are as follows (the origin is at the center of the plate):

$$\textit{Along } x = \pm a/2: \qquad u_1 = u_2 = w_1 = w_2 = w_3 = 0,$$
$$\textit{Along } y = \pm a/2: \qquad u_1 = u_2 = w_3 = 0, \quad M_{22} = M_{12} = 0.$$

BEM meshes with 20 quadratic boundary elements and 25 domain cells are used. The problem is analyzed with different solution procedures, including the total increment method, the Euler method and the simultaneous integral method with and without iterations. The normalized maximum deflection values Z of the present method are plotted in Figure 11 and compared with the finite-strip results [24]. The present results are in good agreement with the references.

6.6. Clamped circular plate

A circular plate is subjected to a uniform distribution load q (see Figure 2 and 6). The perimeter of the plate is restrained from rotation and translation; $u_1 = u_2 = w_1 = w_2 = w_3 = 0$. BEM meshes with 16 quadratic boundary elements and 49 domain cells are used. The normalized maximum deflection values Z of the present method are plotted in

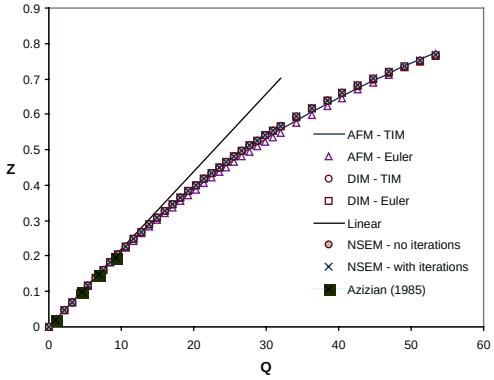

Figure 11. A square plate subjected to a uniform load, q, with two opposite edges clamped and the others simply supported.

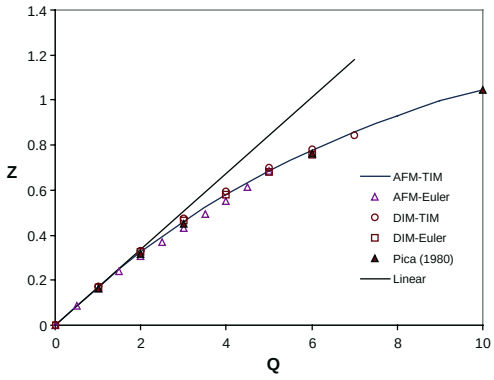

Figure 12. Clamped circular plate subjected to a uniform load q.

Figure 12 and compared with the finite-element results [25]. BEM results are in good agreement with the reference (less than 1% difference). But the results obtained using the approximation-function method with solution procedure involving the Euler method exhibit the largest errors.

6.7. Conclusions

In this paper, boundary-integral equations for large deformation of shear-deformable plates were presented. In the analysis of the geometrically nonlinear plate-bending problem, the domain integrals consist of coupling of the plate-bending and membrane terms. Four different approximation functions were used to calculate the derivatives of the nonlinear terms in the domain integral. All approximations were shown to provide good agreement with finite-element results. Also presented were different solution procedures for the nonlinear problem. Initially, the accuracy and efficiency of the total-increment method and cumulative incremental method were assessed and compared. It was shown that by introducing a relaxation procedure, the numerical results can be improved. Several examples have been presented and comparisons made to demonstrate the accuracy of the proposed method with analytical results and other numerical results. The BEM results are in good agreement with the references. The best nonlinear method and solution procedure for solving large-deflection problems was found to be the combination of the approximate-function method and the total-increment method. One of the advantages of the boundary-element formulation presented for nonlinear problems in this paper is that, once the coefficient matrices have been formed, they can be used in each increment of load without further change. Moreover, the system of equations can be solved fast if the LU-decomposition is employed. Hence, computational time is considerably faster than for the finite-element method which requires updating the stiffness matrices in each increment.

Appendix A. Fundamental solutions

Plate-bending problem

The expressions for the kernels W^*_{ij} and P^*_{ij} are given in [5] as follows:

$$W^*_{\alpha\beta} = \frac{1}{8\pi D(1-\nu)} \left\{ [8B(z) - (1-\nu)(2\log z - 1)]\delta_{\alpha\beta} - [8A(z) + 2(1-\nu)]r_{,\alpha} r_{,\beta} \right\},$$

$$W^*_{\alpha 3} = -W^*_{3\alpha} = \frac{1}{8\pi D}(2\log z - 1) r r_{,\alpha},$$
$$W^*_{33} = \frac{1}{8\pi D(1-\nu)\lambda^2}[(1-\nu)z^2(\log z - 1) - 8\log z], \tag{A1}$$

and

$$P^*_{\gamma\alpha} = \frac{-1}{4\pi r}[(4A(z) + 2zK_1(z) + 1 - \nu)(\delta_{\alpha\gamma} r_{,n} + r_{,\alpha} n_\gamma)$$
$$+(4A(z) + 1 + \nu) r_{,\gamma} n_\alpha - 2(8A(z) + 2zK_1(z) + 1 - \nu) r_{,\alpha} r_{,\gamma} r_{,n}],$$
$$P^*_{\gamma 3} = \frac{\lambda^2}{2\pi}[B(z) n_\gamma - A(z) r_{,\gamma} r_{,n}],$$
$$P^*_{3\alpha} = \frac{-(1-\nu)}{8\pi}\left[\left(2\frac{(1+\nu)}{(1-\nu)}\ln z - 1\right) n_\alpha + 2 r_{,\alpha} r_{,n}\right],$$
$$P^*_{33} = \frac{-1}{2\pi r} r_{,n}. \tag{A2}$$

The expressions for the kernels $W^*_{3j,\theta}$ and $W^*_{33,\theta\gamma}$ are written as

$$W^*_{3\alpha,\theta} = -\frac{1}{8\pi D}\left(2 r_{,\theta} r_{,\alpha} + (2\log z - 1)\delta_{\alpha\theta}\right),$$
$$W^*_{33,\theta} = \frac{1}{8\pi D\lambda} r_{,\theta}\left[(2\log z - 1) - \frac{8}{z(1-\nu)}\right],$$
$$W^*_{33,\theta\gamma} = \frac{1}{8\pi D}\left[(2\log z - 1) + 2 r_{,\theta} r_{,\gamma} - \frac{8(\delta_{\theta\gamma} - 2 r_{,\theta} r_{,\gamma})}{z^2(1-\nu)}\right]. \tag{A3}$$

The expression for the kernels $P^*_{3j,\theta}$ is written as

$$P^*_{3\alpha,\theta} = \frac{-(1-\nu)}{4\pi r}\left[\left(\frac{(1+\nu) r_{,\theta}}{(1-\nu)}\right) n_\alpha + r_{,\alpha} n_\theta - 3 r_{,\theta} r_{,n} r_{,\alpha} + \delta_{\alpha\theta} r_{,n}\right],$$
$$P^*_{33,\theta} = \frac{-1}{2\pi r^2}\left[n_\theta - 2 r_{,\theta} r_{,n}\right]. \tag{A4}$$

The expressions for W^*_{ijk}, P^*_{ijk} and $Q^*_{i\beta}$ are [5]:

$$W^*_{\alpha\beta\gamma} = \frac{1}{4\pi r}[(4A(z) + 2zK_1(z) + 1 - \nu)(\delta_{\beta\gamma} r_{,\alpha} + \delta_{\alpha\gamma} r_{,\beta})$$
$$-2(8A(z) + 2zK_1(z) + 1 - \nu) r_{,\alpha} r_{,\beta} r_{,\gamma} + (4A(z) + 1 + \nu)\delta_{\alpha\beta} r_{,\gamma}],$$
$$W^*_{\alpha\beta 3} = \frac{-(1-\nu)}{8\pi}\left[\left(2\frac{(1+\nu)}{(1-\nu)}\log z - 1\right)\delta_{\alpha\beta} + 2 r_{,\alpha} r_{,\beta}\right],$$
$$W^*_{3\beta\gamma} = \frac{\lambda^2}{2\pi}[B(z)\delta_{\gamma\beta} - A(z) r_{,\gamma} r_{,\beta}],$$
$$W^*_{3\beta 3} = \frac{1}{2\pi r} r_{,\beta}, \tag{A5}$$

$$
\begin{aligned}
P^*_{\alpha\beta\gamma} &= \frac{D(1-\nu)}{4\pi r^2}\{(4A(z)+2zK_1(z)+1-\nu)(\delta_{\gamma\alpha}n_\beta+\delta_{\gamma\beta}n_\alpha)\\
&\quad +(4A(z)+1+3\nu)\delta_{\alpha\beta}n_\gamma-(16A(z)+6zK_1(z)+z^2K_0(z)+2-2\nu)\\
&\quad \times[(n_\alpha r_{,\beta}+n_\beta r_{,\alpha})r_{,\gamma}+(\delta_{\gamma\alpha}r_{,\beta}+\delta_{\gamma\beta}r_{,\alpha})r_{,n}]\\
&\quad -2(8A(z)+2zK_1(z)+1+\nu)(\delta_{\alpha\beta}r_{,\gamma}r_{,n}+n_\gamma r_{,\alpha}r_{,\beta})\\
&\quad +4(24A(z)+8zK_1(z)+z^2K_0(z)+2-2\nu)r_{,\alpha}r_{,\beta}r_{,\gamma}r_{,n}\},\\
P^*_{\alpha\beta 3} &= \frac{D(1-\nu)\lambda^2}{4\pi r}[(2A(z)+zK_1(z))(r_{,\beta}n_\alpha+r_{,\alpha}n_\beta)\\
&\quad -2(4A(z)+zK_1(z))r_{,\alpha}r_{,\beta}r_{,n}+2A(z)\delta_{\alpha\beta}r_{,n}],\\
P^*_{3\beta\gamma} &= \frac{-D(1-\nu)\lambda^2}{4\pi r}[(2A(z)+zK_1(z))(\delta_{\gamma\beta}r_{,n}+r_{,\gamma}n_\beta)\\
&\quad +2A(z)n_\gamma r_{,\beta}-2(4A(z)+zK_1(z))r_{,\gamma}r_{,\beta}r_{,n}],\\
P^*_{3\beta 3} &= \frac{D(1-\nu)\lambda^2}{4\pi r^2}[(z^2B(z)+1)n_\beta-(z^2A(z)+2)r_{,\beta}r_{,n}],
\end{aligned}
\tag{A6}
$$

$$
\begin{aligned}
Q^*_{\alpha\beta} &= \frac{-r}{64\pi}\{(4\log z-3)[(1-\nu)(r_{,\beta}n_\alpha+r_{,\alpha}n_\beta)+(1+3\nu)\delta_{\alpha\beta}r_{,n}]\\
&\quad +4[(1-\nu)r_{,\alpha}r_{,\beta}+\nu\delta_{\alpha\beta}]r_{,n}\},\\
Q^*_{3\beta} &= \frac{1}{8\pi}[(2\log z-1)n_\beta+2r_{,\beta}r_{,n}],
\end{aligned}
\tag{A7}
$$

where

$$
A(z)=K_0(z)+\frac{2}{z}\left[K_1(z)-\frac{1}{z}\right],\quad B(z)=K_0(z)+\frac{1}{z}\left[K_1(z)-\frac{1}{z}\right] \tag{A8}
$$

and $K_0(z)$ and $K_1(z)$ are modified Bessel functions of the second kind [26], $z=\lambda r$, λ is the shear factor defined in Section 2, r is the distance between the source and the field points, $r_{,\alpha}=r_\alpha/r$, where $r_\alpha=x_\alpha(\mathbf{x})-x_\alpha(\mathbf{x}')$ and $r_{,n}=r_{,\alpha}n_\alpha$.

Expanding the modified Bessel functions for small arguments, we find

$$
\begin{aligned}
K_0(z) &= \left[-\gamma-\log\left(\frac{z}{2}\right)\right]+\left[-\gamma+1-\log\left(\frac{z}{2}\right)\right]\frac{(z^2/4)}{(1!)^2}\\
&\quad +\left[-\gamma+1+\frac{1}{2}-\log\left(\frac{z}{2}\right)\right]\frac{(z^2/4)^2}{(2!)^2}\\
&\quad +\left[-\gamma+1+\frac{1}{2}+\frac{1}{3}-\log\left(\frac{z}{2}\right)\right]\frac{(z^2/4)^3}{(3!)^2}+\cdots,
\end{aligned}
\tag{A9}
$$

$$
\begin{aligned}
K_1(z) &= \frac{1}{z}-\left[-\gamma+\frac{1}{2}-\log\left(\frac{z}{2}\right)\right]\frac{(z^2/4)^{1/2}}{0!1!}-\left[-\gamma+1+\frac{1}{4}-\log\left(\frac{z}{2}\right)\right]\frac{(z^2/4)^{3/2}}{1!2!}\\
&\quad -\left[-\gamma+1+\frac{1}{2}+\frac{1}{6}-\log\left(\frac{z}{2}\right)\right]\frac{(z^2/4)^{5/2}}{2!3!}+\cdots,
\end{aligned}
\tag{A10}
$$

where $\gamma=0{\cdot}5772156649$ is the Euler constant. Substituting equations (A9) and (A10) in equation (A8) and taking the limit as $r\to 0$; we find

$$
\lim_{r\to 0}A(z)=\frac{-1}{2},\quad \lim_{r\to 0}B(z)=-\frac{1}{2}\left[\lim_{r\to 0}\log\left(\frac{z}{2}\right)+\gamma+\frac{1}{2}\right]. \tag{A11}
$$

It can be seen that $A(z)$ is a smooth function, whereas $B(z)$ is a weakly singular $O(\log r)$ function. Therefore, W_{ij}^* is weakly singular and P_{ij}^* has a strong (Cauchy principal value) singularity $O(1/r)$.

In this work, the modified Bessel functions are evaluated using polynomial approximations given in [26, Chapter 10].

Appendix B. Two-dimensional plane stress problem

The expressions for the kernels $U_{\theta\alpha}^*$ and $T_{\theta\alpha}^*$ (Kelvin solution) are well known for two-dimensional plane stress problems, and are given as [27] :

$$U_{\theta\alpha}^* = \frac{1}{4\pi B(1-\nu)}\left[(3-\nu)\log\left(\frac{1}{r}\right)\delta_{\theta\alpha} + (1+\nu)\, r_{,\theta} r_{,\alpha}\right], \tag{B1}$$

$$\begin{aligned} T_{\theta\alpha}^* = -\frac{1}{4\pi r}\{ & r_{,n}\left[(1-\nu)\,\delta_{\theta\alpha} + 2(1+\nu)\, r_{,\theta} r_{,\alpha}\right] \\ & + (1-\nu)\left[n_\theta r_{,\alpha} - n_\alpha r_{,\theta}\right]\}, \end{aligned} \tag{B2}$$

where $U_{\theta\alpha}^*$ are weakly singular kernels of order $O(\log\frac{1}{r})$, and $T_{\theta\alpha}^*$ are strongly singular in order $O(1/r)$.

The kernels $U_{\alpha\beta\gamma}^*$ and $T_{\alpha\beta\gamma}^*$ are given by

$$U_{\alpha\beta\gamma}^* = \frac{1}{4\pi r}\left[(1-\nu)\left(\delta_{\gamma\alpha} r_{,\beta} + \delta_{\gamma\beta} r_{,\alpha} - \delta_{\alpha\beta} r_{,\gamma}\right) + 2(1+\nu)\, r_{,\alpha} r_{,\beta} r_{,\gamma}\right], \tag{B3}$$

$$\begin{aligned} T_{\alpha\beta\gamma}^* = \frac{B(1-\nu)}{4\pi r^2}\{ & 2r_{,n}\left[(1-\nu)\,\delta_{\alpha\beta} r_{,\gamma} + \nu\left(\delta_{\gamma\alpha} r_{,\beta} + \delta_{\gamma\beta} r_{,\alpha}\right) - 4(1+\nu)\, r_{,\alpha} r_{,\beta} r_{,\gamma}\right] \\ & + 2\nu\left(n_\alpha r_{,\beta} r_{,\gamma} + n_\beta r_{,\alpha} r_{,\gamma}\right) + (1-\nu)\left(2n_\gamma r_{,\alpha} r_{,\beta} + n_\beta \delta_{\alpha\gamma} + n_\alpha \delta_{\beta\gamma}\right) \\ & - (1-3\nu)\, n_\gamma \delta_{\alpha\beta}\}. \end{aligned} \tag{B4}$$

The Kelvin functions $U_{\theta\alpha,\beta}^*$ and $T_{\theta\alpha,\beta}^*$ are written as

$$\begin{aligned} U_{\theta\alpha,\beta}^* = & \frac{1}{4\pi B(1-\nu) r}\left[(1+\nu)\left(\delta_{\theta\beta} + \delta_{\alpha\beta} - 2r_{,\theta} r_{,\alpha} r_{,\beta}\right) - (3-\nu)\, r_{,\beta}\delta_{\theta\alpha}\right] \\ & \left[(1-\nu)\left(\delta_{\gamma\alpha} r_{,\beta} + \delta_{\gamma\beta} r_{,\alpha} - \delta_{\alpha\beta} r_{,\gamma}\right) + 2(1+\nu)\, r_{,\alpha} r_{,\beta} r_{,\gamma}\right], \end{aligned} \tag{B5}$$

$$\begin{aligned} T_{\theta\alpha,\beta}^* = -\frac{1}{4\pi r^2}\{ & (n_\beta - 2r_{,\beta} r_{,n})\left[(1-\nu)\,\delta_{\theta\alpha} + 2(1+\nu)\, r_{,\theta} r_{,\alpha}\right] \\ & + r_{,\beta} r_{,n}\left[(1-\nu)\,\delta_{\theta\alpha} + 2(1+\nu)\, r_{,\theta} r_{,\alpha}\right] \\ & + r_{,n}\left[2(1+\nu)\left((\delta_{\theta\beta} - r_{,\theta} r_{,\beta}) r_{,\alpha} + (\delta_{\alpha\beta} - r_{,\alpha} r_{,\beta}) r_{,\theta}\right)\right] \\ & + (1-\nu)\left[n_\theta(\delta_{\alpha\beta} - r_{,\alpha} r_{,\beta}) - n_\alpha(\delta_{\theta\beta} - r_{,\theta} r_{,\beta}) - r_{,\beta}(n_\theta r_{,\alpha} - n_\alpha r_{,\theta})\right]\}. \end{aligned} \tag{B6}$$

The kernel $U_{\alpha\beta\gamma,\theta}^*$ is given by

$$\begin{aligned} U_{\alpha\beta\gamma,\theta}^* = \frac{1}{4\pi r^2}\left[\right. & (1-\nu)\left(\delta_{\gamma\alpha}(\delta_{\beta\theta} - 2r_{,\beta} r_{,\theta})\right) \\ & + (1-\nu)\left(\delta_{\gamma\beta}(\delta_{\alpha\theta} - 2r_{,\alpha} r_{,\theta}) - \delta_{\alpha\beta}(\delta_{\gamma\theta} - 2r_{,\gamma} r_{,\theta})\right) \\ & + 2(1+\nu)\left(\delta_{\alpha\theta} + \delta_{\beta\theta} + \delta_{\gamma\theta} - 3r_{,\alpha} r_{,\beta} r_{,\gamma} r_{,\theta}\right)\left.\right]. \end{aligned} \tag{B7}$$

References

1. S. Levy, Bending of rectangular plate with large deflections. *NACA TN-846* (1942) 19 pp.
2. S. Levy, Square plate with clamped edges under normal pressure producing large deflections. *NACA TN-847* (1942) 14 pp.
3. H.M. Berger, A new approach to the analysis of large deflections of plates. *J. Appl. Mech.* 22 (1955) 465–472.
4. M.A. Jaswon, M. Maiti and G.T. Symm, Numerical biharmonic analysis and some applications. *Int. J. Solids Structs.* 3 (1967) 309–332.
5. F. Vander Ween, Application of the boundary integral equation method to Reissner's plate model. *Int. J. Numerical Methods Eng.* 18 (1982) 1–10.
6. V.J. Karam and J.C.F. Telles, On boundary element for Reissner's plate theory. *Engng. Anal.* 5 (1988) 21–27.
7. Y. Rashed, M.H. Aliabadi and C.A. Brebbia, The boundary element method for thick plates on a Winkler foundation. *Int. J. Num. Methods Engng.* 41 (1998) 1435–1462.
8. Y. Rahsed, M.H. Aliabadi and C.A. Brebbia, A boundary-element formulation for a Reissner plate on a Pasternak foundation. *Comp. Struct.* 70 (1999) 515–532.
9. P.H. Wen, M.H. Aliabadi and A. Young, Application of dual reciprocity method to plates and shells. *Engng. Anal. Bound. Elem.* 24 (2000) 583–590.
10. M. Tanaka, Large deflection analysis of thin elastic plates. P.K. Banerjee (ed.), *Development in Boundary Element Methods.* Oxford: Elsevier Applied Science Publishers 3 (1984) 115–136.
11. N. Kamiya and Y. Sawaki, An integral equation approach to finite deflection of elastic plates. *Int. J. Non-lin. Mech.* 17 (1982) 187–194.
12. T.Q. Ye, and Y.J., Finite deflection analysis of elastic plate by the boundary element method. *App. Math. Model.* 9 (1985) 183–188.
13. X.Y. Lei, M.K. Huang and X.X. Wang, Geometrically nonlinear analysis of a Reissner type by the boundary element method. *Comp. Struct* 37 (1990) 911–916.
14. X.Q. He and Q.H. Qin, Nonlinear analysis of Reissner's plate by the variational approaches and boundary element methods. *Appl. Math. Model.* 17 (1993) 149–155.
15. J. Sladek and V. Sladek, The BIE analysis of the Berger equation. *Ingenieur-Archiv* 53 (1983) 385–397.
16. J.T. Katsikadelis, Large deflection analysis of plates on elastic foundation by the boundary element method. *Int. J. Solids Struct.* 27 (1991) 1867–1878.
17. S.N. Atluri and D.S. Pipkins, Large deformation analysis of plates and shells. In: D.E. Beskos (ed), *Boundary Element Analysis of Plates and Shells*. Berlin: Springer-Verlag (1991) pp. 142–165.
18. Y.F. Rashed, M.H. Aliabadi and C.A. Brebbia, Hyper-singular boundary element formulation for Reissner plates. *Int. J. Solids Struct.* 35 (1998) 2229–2249.
19. P.H. Wen, M.H. Aliabadi and A. Young, Stiffened cracked plates analysis by dual boundary element method. *Int. J. Fracture* 106 (2000) 245–258.
20. T. Dirgantara and M.H. Aliabadi, Stress intensity factors for cracks in thin plates. *Engng. Fracture Mech.* 69 (2002) 1465–1486.
21. M.H. Aliabadi, *Plate Bending Analysis with Boundary Elements*, *Advances in Boundary Element Series*. Southampton: Computational Mechanics Publications (1998) 352 pp.
22. M.H. Aliabadi, *The Boundary Element Method, Vol. 2, Application in Solids and Structures*. Chichester: Wiley (2002) 580 pp.
23. A.N. Palazotto and S.T. Dennis, *Nonlinear Analysis of Shell Structures*. Washington DC: Americans Institute of Aeronautics and Astronautics, Inc. (1992), 251 pp.
24. Z.G. Azizian and D.J. Dawe, Geometrical nonlinear analysis of rectangular Midlin plates using finite strip method. *Comp. Structs.* 21 (1985) 423–436.
25. R. Pica, R.D. Wood and E. Hinton, Finite element analysis of geometrically nonlinear plate behaviour using Mindlin formulation. *Comp. Structs.* 11 (1980) 203–215.
26. M. Abramowitz and I.A. Stegun (eds.), *Handbook of mathematical functions*. New York: Dover (1965) 1033 pp.
27. M.H. Aliabadi and D.P. Rooke, *Numerical Fracture Mechanics*. Dordrecht, The Netherlands: Kluwer Academic Publishers (1991) 300 pp.